JOURNAL OF MOLECULAR SPECTROSCOPY 99, 35–46 (1983)

The Millimeter and Submillimeter Spectrum of CN in Its First Four Vibrational States[1]

DAVID D. SKATRUD AND FRANK C. DE LUCIA

Department of Physics, Duke University, Durham, North Carolina 27706

GEOFFREY A. BLAKE

Department of Chemistry, California Institute of Technology, Pasadena, California 91125

AND

K. V. L. N. SASTRY

Department of Physics, University of New Brunswick, Fredericton, N.B., Canada E3B 5A3

The rotational absorption frequencies of 65 new lines in the millimeter and submillimeter region of the spectrum have been measured for the CN radical in its ground electronic state. These measurements were made in a low pressure glow discharge of methane and nitrogen and include 25 lines from the $v = 2$ and $v = 3$ vibrational states, in addition to 40 lines from $v = 0$ and $v = 1$. The Dunham constants, as well as the spin-rotation and hyperfine constants of these four vibrational states, were calculated by means of a global nonlinear least squares fit of these data.

I. INTRODUCTION

The CN radical is one of the most extensively studied spectroscopic species (*1*). However, the extreme chemical reactivity of CN has made observation of its rotational spectra by microwave absorption techniques difficult. In fact, the first detection of the pure rotation spectrum of CN was via the radio astronomical observations of Penzias *et al.* (*2*). They measured the seven strongest lines due to the fine and hyperfine splitting of the $N = 0 \rightarrow 1$ transitions in the ground vibrational and electronic state. The first laboratory detection was subsequently made by Dixon and Woods (*3*) in which they measured the same seven lines of the $N = 0 \rightarrow 1$ transitions in both the $v = 0$ and $v = 1$ vibrational states. These were observed with several hours of integration in a glow discharge of cyanogen and nitrogen. The increase in the absorption coefficient with frequency ($\sim \nu^3$) and the use of sensitive millimeter and submillimeter spectroscopic techniques made possible our measurements of 65 new rotational absorption lines. These transitions, ranging in frequency from 220 to 453 GHz, include 25 from the $v = 2$ and $v = 3$ vibrational states in addition to 40 from $v = 0$ and $v = 1$. In the conditions of our experiments, we found the population of each suc-

[1] Work Supported by: NASA Grant No. NAGW-189.

0022-2852/83 $3.00

cessive vibrational state to decrease by about a factor of three. A global nonlinear least squares fit of these data was used to calculate the Dunham constants Y_{01}, Y_{11}, Y_{21}, Y_{02}, and Y_{12} and the fine and hyperfine constants for each of the vibrational states.

II. EXPERIMENTAL

Our original observation of CN was in a diagnostic study of the FIR HCN laser discharge plasma. CN is of interest in this system due to the conjecture that it is the chemical precursor of the lasing HCN. The laser glow discharge contained a 1:1 mixture of N_2 and CH_4 at a pressure of 60 mTorr and discharge current of 200 mA. The fraction of the power absorbed was used to calculate an approximate partial pressure of .01 mTorr for CN in the ground vibrational and electronic state. The relative ease with which this measurement was made on the laser diagnostic system served as the impetus for the spectroscopic study of CN in a high sensitivity system.

We have previously described the details of our millimeter and submillimeter spectroscopic technique (*4*). Briefly, the radiation was produced by a crystal harmonic generator driven by a reflex klystron operating in the 55-GHz region, focused through the cell via quasi-optical techniques, and detected by 1.5-K InSb detector. The klystron was phase-locked to a known harmonic of a frequency synthesizer (referenced to WWVB) capable of phase continuous frequency sweeps. The data was collected in a digital signal averager and processed and measured in a computer.

The glow discharge absorption cell was a 5-ft length of 4-in.-diameter pyrex pipe with hollow cylindrical electrodes at both ends. The cell was wrapped with a solenoid which was used for sine wave Zeeman modulation at 2.6 kHz with detection at 5.2 kHz. The lock-in time constant was 100 msec and the frequency sweep time was 10 sec. The frequencies of forward–reverse frequency sweeps were averaged to cancel the time-constant induced shift in the observed frequency. Because the modulation of the index of refraction of a plasma by magnetic modulation is substantially smaller at short millimeter and submillimeter wavelengths than it is at longer wavelengths (*5*), we were able to signal average for arbitrary lengths of time without encountering base line problems. The integration times ranged from 1 min (3 up–down sweeps) for intense $v = 0$ lines to 40 min (120 up–down sweeps) for partially forbidden $v = 3$ lines. Figures 1 and 2 show typical data. A number of lines were also measured with source modulation to check for frequency shifts from the Zeeman modulation and no statistically significant shifts were found. Several transitions, particularly $\Delta J = 0$, $\Delta F = 0$ lines, were broadened by the earth's field to the extent they split into resolvable doublets. The enclosure of the cell in a μ-metal magnetic shield eliminated this problem.

N_2 and CH_4 were retained from the laser experiment as the precursor gases since they gave a relatively strong spectrum and because of the convenience of working with nontoxic gases. For the spectroscopic experiment, the mixture was optimized at the N_2:CH_4 ratio of 8:1 and at a pressure of approximately 40 mTorr. Unfortunately, we were not able to make an absolute measurement of the flow rate, although we did note that concentration of CN maximized at a flow rate significantly less than that with the diffusion pumped unthrottled. Our power supply limited us to a 185-

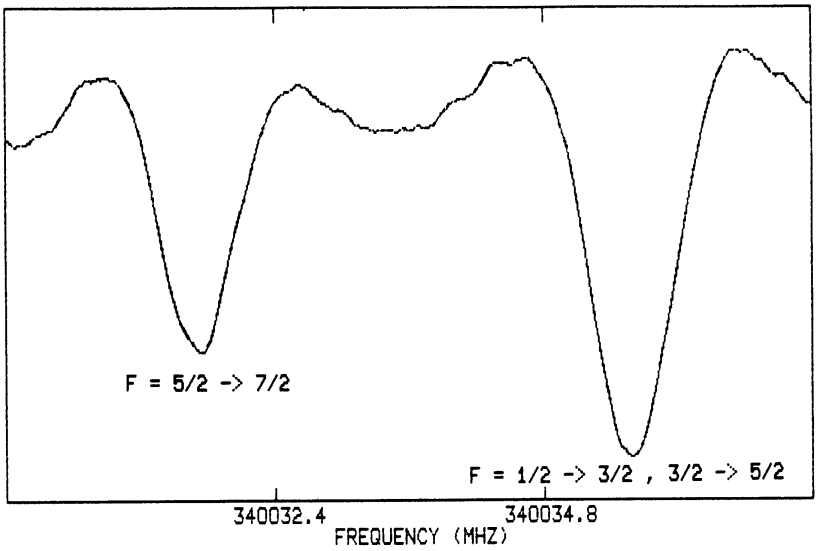

FIG. 1. The hyperfine structure components of the $N = 2 \rightarrow 3$, $J = 3/2 \rightarrow 5/2$ transition of CN in its ground vibrational state.

mA (850 V) discharge, although this current was less than optimal. Since both of the precursor gases have significant vapor pressure at liquid nitrogen temperature, it was possible to cool the discharge cell. It was found that cooling initially increased the signals by about a factor of two, but that further cooling to nitrogen temperature reduced the observed signals by a factor of three. Although all of our measurements were facilely made in an ambient cell, cooling to this optimum intermediate temperature would, of course, be beneficial.

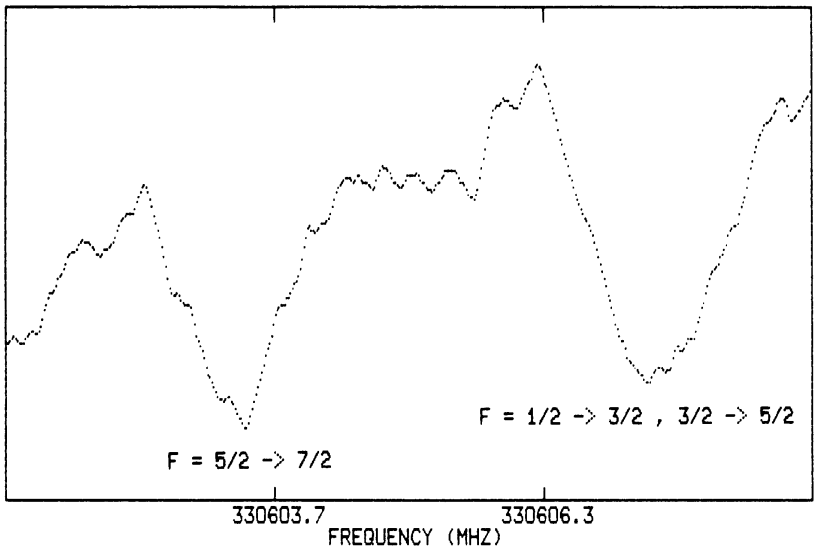

FIG. 2. The hyperfine structure components of the $N = 2 \rightarrow 3$, $J = 3/2 \rightarrow 5/2$ transition of CN in its $v = 3$ excited vibrational state.

III. THEORY

The ground electronic state of CN is $^2\Sigma$. Thus, each rotational energy level is split into a doublet by the spin–rotation interaction. The nitrogen nucleus has spin one; consequently each of these components is further split into a triplet by nuclear magnetic and quadrupole interactions. The basic theory of these systems is well established. In CN, $E_r \gg E_{sr} \gg E_{hfs}$, so Hund's case b is the most appropriate basis in which to evaluate the matrix elements. This corresponds to the coupling scheme

$$\mathbf{N} + \mathbf{S} = \mathbf{J},$$
$$\mathbf{J} + \mathbf{I} = \mathbf{F}. \tag{1}$$

The zero field Hamiltonian for the rotational energies may be written (*3*)

$$H = H_r + H_{sr} + H_{hfs} \tag{2}$$

where

$$H_r = Y_{01}N(N+1) + Y_{11}(v+1/2)N(N+1) + Y_{21}(v+1/2)^2N(N+1) + Y_{02}N^2(N+1)^2 + Y_{12}(v+1/2)N^2(N+1)^2$$

$$H_{sr} = \gamma_v \mathbf{N}\cdot\mathbf{S}$$

and

$$H_{hfs} = b_v \mathbf{I}\cdot\mathbf{S} + c_v I_z S_z + \frac{eqQ_v}{4} T_0^{(2)}(\mathbf{I}).$$

In these equations **N** is the angular momentum of the rotation of the molecular frame, **S** is the electron spin, **I** is the nitrogen nuclear spin, z is the molecular axis, and $T_0^{(2)}(\mathbf{I})$ is the molecule fixed zeroth component of the quadrupole moment tensor. Here we have identified the coefficients of the power series in v and N with the Dunham constants, $Y_{l,m}$ rather than with the mechanical equilibrium constants B_e, α_e, etc. Even so, because CN is $^2\Sigma$ these $Y_{l,m}$ should be viewed as effective constants that may be contaminated by admixtures with other electronic states. The spin-rotation fine structure constants γ_v, the magnetic hyperfine constants b_v and c_v, and the electric quadrupole constants eqQ_v are left as functions of vibrational state. We have not included the nuclear spin-rotation interaction because the above terms are sufficient for a fit to within experimental uncertainty. The extensive set of rotational data that we have obtained for four vibrational states has allowed us to fit for the five Dunham constants rather than the four individual sets of B_v and D_v, thereby reducing the number of parameters by three.

There are a number of ways to evaluate the matrix elements of the fine and hyperfine interactions. We have used the results of a derivation by Dixon and Woods (*3*) in our calculations. The rotational matrix elements are diagonal in N and are much larger than any other interaction; so, to an excellent approximation, elements off diagonal in N can be neglected. The Hamiltonian matrix then factors into 2×2 F blocks that were diagonalized in our analysis.

TABLE I

Observed Rotational Frequencies (MHz) for $X^2\Sigma^+$ CN

Transition N J F → N' J' F'	Weight	Observed Frequency	Obs.-Calc.	Transition N J F → N' J' F'	Weight	Observed Frequency	Obs.-Calc.
v=0							
0 1/2 3/2 — 1 1/2 1/2	1	113144.190[a]	0.068	2 5/2 3/2 — 3 5/2 3/2	1	339446.777	-0.002
0 1/2 1/2 — 1 1/2 3/2	1	113170.535[a]	0.033	2 5/2 5/2 — 3 5/2 5/2	1	339475.904	0.009
0 1/2 3/2 — 1 1/2 3/2	1	113191.325[a]	0.038	2 5/2 7/2 — 3 5/2 7/2	1	339516.658	-0.032
0 1/2 1/2 — 1 3/2 3/2	1	113488.142[a]	0.016	2 3/2 5/2 — 3 5/2 5/2	1	340008.097	-0.062
0 1/2 3/2 — 1 3/2 5/2	1	113490.985[a]	0.042	2 3/2 3/2 — 3 5/2 3/2	1	340019.602	-0.023
0 1/2 1/2 — 1 3/2 1/2	1	113499.643[a]	0.014	2 3/2 5/2 — 3 5/2 7/2	1	340031.544	-0.023
0 1/2 3/2 — 1 3/2 3/2	1	113508.934[a]	0.023	2 3/2 1/2 — 3 5/2 3/2 2 3/2 3/2 — 3 5/2 5/2	1	340035.408[b]	-0.027
1 3/2 3/2 — 2 3/2 3/2	1	226314.540	-0.012				
1 3/2 5/2 — 2 3/2 5/2	1	226359.871	-0.016	2 5/2 5/2 — 3 7/2 7/2 2 5/2 7/2 — 3 7/2 9/2	1	340247.770[b]	0.001
1 1/2 3/2 — 2 3/2 3/2	1	226632.190	0.014				
1 1/2 3/2 — 2 3/2 5/2	1	226659.575	0.032	2 5/2 5/2 — 3 7/2 5/2	1	340261.818	0.030
1 1/2 1/2 — 2 3/2 1/2	1	226663.703	0.018	2 5/2 7/2 — 3 7/2 7/2	1	340265.025	0.013
1 1/2 1/2 — 2 3/2 3/2	1	226679.382	0.041	3 5/2 7/2 — 4 7/2 9/2	1	453390.057	0.045
1 3/2 3/2 — 2 5/2 5/2	1	226874.166	-0.017	3 5/2 3/2 — 4 7/2 5/2 3 5/2 5/2 — 4 7/2 7/2	1	453391.668[b]	0.018
1 3/2 5/2 — 2 5/2 7/2	1	226874.745	-0.019				
1 3/2 1/2 — 2 5/2 3/2	1	226875.897	0.001	3 7/2 7/2 — 4 9/2 9/2 3 7/2 9/2 — 4 9/2 11/2	1	453606.740[b]	0.029
1 3/2 3/2 — 2 5/2 3/2	1	226887.352	-0.047				
1 3/2 5/2 — 2 5/2 5/2	1	226892.119	-0.032				
v=1							
0 1/2 3/2 — 1 1/2 1/2	1	112101.674[a]	0.077	1 3/2 1/2 — 2 5/2 3/2	1	224785.301	-0.054
0 1/2 1/2 — 1 1/2 3/2	1	112128.989[a]	-0.008	1 3/2 3/2 — 2 5/2 3/2	1	224796.360	-0.040
0 1/2 3/2 — 1 1/2 3/2	1	112148.510[a]	0.035	1 3/2 5/2 — 2 5/2 5/2	1	224800.896	-0.022
0 1/2 1/2 — 1 3/2 3/2	1	112442.813[a]	0.021	2 3/2 5/2 — 3 5/2 5/2	1	336875.457	-0.056
0 1/2 3/2 — 1 3/2 5/2	1	112445.020[a]	0.028	2 3/2 3/2 — 3 5/2 3/2	1	336886.753	-0.064
0 1/2 1/2 — 1 3/2 1/2	1	112453.891[a]	0.054	2 3/2 5/2 — 3 5/2 7/2	1	336898.488	-0.025
0 1/2 3/2 — 1 3/2 3/2	1	112462.282[a]	0.012	2 3/2 1/2 — 3 5/2 3/2 2 3/2 3/2 — 3 5/2 5/2	1	336902.422[b]	0.001
1 3/2 3/2 — 2 3/2 3/2	0.5	224230.333	-0.069				
1 3/2 5/2 — 2 3/2 5/2	0.5	224274.624	-0.036	2 5/2 5/2 — 3 7/2 7/2 2 5/2 7/2 — 3 7/2 9/2	1	337112.397[b]	0.037
1 1/2 3/2 — 2 3/2 3/2	1	224544.192	-0.005				
1 1/2 3/2 — 2 3/2 5/2	1	224571.192	0.015	2 5/2 5/2 — 3 7/2 5/2	1	337125.917	-0.043
1 1/2 1/2 — 2 3/2 1/2	1	224575.648	0.058	2 5/2 7/2 — 3 7/2 7/2	1	337129.028	-0.049
1 1/2 1/2 — 2 3/2 3/2	1	224591.097	0.022				
v=2							
1 1/2 3/2 — 2 3/2 3/2	0.5	222449.743	0.001	1 3/2 5/2 — 2 5/2 5/2	0.5	222702.996	-0.020
1 1/2 3/2 — 2 3/2 5/2	1	222476.403	0.011	2 3/2 5/2 — 3 5/2 5/2	1	333733.144	0.037
1 1/2 1/2 — 2 3/2 1/2	1	222481.049	-0.014	2 3/2 3/2 — 3 5/2 3/2	1	333744.249	0.013
1 1/2 1/2 — 2 3/2 3/2	0.5	222496.503	0.057	2 3/2 5/2 — 3 5/2 7/2	1	333755.759	0.012
1 3/2 3/2 — 2 5/2 5/2 1 3/2 5/2 — 2 5/2 7/2	1	222686.588[b]	0.051	2 3/2 1/2 — 3 5/2 3/2 2 3/2 3/2 — 3 5/2 5/2	1	333759.727[b]	0.022
1 3/2 1/2 — 2 5/2 3/2	1	222688.082	0.017	2 5/2 5/2 — 3 7/2 5/2	1	333980.111	0.002
1 3/2 3/2 — 2 5/2 3/2	0.5	222698.742	0.079	2 5/2 7/2 — 3 7/2 7/2	1	333983.194	0.013

TABLE I. (continued)

Transition N J F	N' J' F'	Weight	Observed Frequency	Obs.-Calc.	Transition N J F	N' J' F'	Weight	Observed Frequency	Obs.-Calc.
v=3									
1 1/2 3/2	2 3/2 3/2	0.5	220348.754	0.038	1 3/2 3/2	2 5/2 3/2	0.5	220594.476	0.055
1 1/2 3/2	2 3/2 5/2	0.5	220375.080	-0.065	1 3/2 5/2	2 5/2 5/2	0.5	220598.361	-0.051
1 1/2 1/2	2 3/2 1/2	0.5	220380.030	-0.068	2 3/2 5/2	3 5/2 7/2	0.5	330603.183	-0.022
1 1/2 1/2	2 3/2 3/2	0.5	220395.322	0.084	2 3/2 1/2	3 5/2 3/2	0.5	330607.123[b]	-0.065
1 3/2 3/2	2 5/2 5/2	0.5	220582.388[b]	-0.102	2 3/2 3/2	3 5/2 5/2			
1 3/2 5/2	2 5/2 7/2				2 5/2 5/2	3 7/2 7/2	0.5	330811.612	0.118
1 3/2 1/2	2 5/2 3/2	0.5	220583.953	-0.118	2 5/2 7/2	3 7/2 9/2			

[a] Observed transition frequencies from reference 3.

[b] These unresolved lines were entered into the fit by using the intensity weighted hyperfine splittings predicted by the rest of the data.

IV. ANALYSIS AND DISCUSSION

We have included the 14 $v = 0$ and $v = 1$ frequencies measured by Dixon and Woods in our analysis. The observed frequencies, along with the residuals from this nonlinear least squares fit, are listed in Table I. The variance of the fit is 40 kHz, which is within the experimental uncertainty of the measurements. Somewhat better fits and lower rms deviations can be obtained by fitting the vibrational states individually, but the redundancy of these individual fits is smaller and these better fits may be due to the statistics of small numbers. As indicated in the table, 17 of the frequencies have been assigned a statistical weight of 1/2 relative to the rest of the data. This was done because these lines had significantly smaller signal to noise ratios. The derived constants and their uncertainties are listed in Table II. In some cases the uncertainties for constants calculable from the $N = 0 \rightarrow 1$ data are comparable to or slightly larger than the uncertainties calculated in Ref. (*3*). This is not surprising since the fits of seven data points to six adjustable parameters have limited statistical significance. Figures (*3*)–(*6*) show the variation of the fine and hyperfine constants with vibrational state. Although it would be possible to fit these to an expansion in v similar to the Dunham expansion of B, we have fitted each vibrational state individually. Inspection of these figures shows a smooth monotonic progression at the 1σ level for all except the quadrupole coupling constants.

Since accurate rest frequencies are of interest to the astronomical community, we have calculated frequencies for all transitions in $v = 0$, 1, 2, and 3 below 400 GHz. These frequencies and the relative intensities of the fine and hyperfine transitions are tabulated in Table III. The relative intensities were computed from (*6*)

$$\langle N'SJ'IF' \| \mu^{(1)} \| NSJIF \rangle \propto [(2J+1)(2J'+1)(2F+1)(2F'+1)]^{1/2} \begin{Bmatrix} N' & J' & S \\ J & N & 1 \end{Bmatrix} \begin{Bmatrix} J' & F' & I \\ F & J & 1 \end{Bmatrix}. \quad (3)$$

TABLE II

Spectral Constants (MHz) of $X^2\Sigma^+$ CN for $v = 0$, 1, 2, and 3

	Value	σ		Value	σ
γ_{01}	56954.0231	0.0053	γ_2	212.316	0.029
γ_{11}	-520.7118	0.0057	b_2	-32.489	0.042
γ_{21}	-0.8230	0.0013	c_2	60.93	0.11
γ_{02}	-0.19137	0.00021	eqQ_2	-1.010	0.048
γ_{12}	-0.00061	0.00018	γ_3	209.388	0.037
γ_0	217.4993	0.0068	b_3	-31.869	0.066
b_0	-33.987	0.016	c_3	61.18	0.13
c_0	60.390	0.046	eqQ_3	-1.195	0.092
eqQ_0	-1.270	0.039			
γ_1	215.070	0.012			
b_1	-33.185	0.022			
c_1	60.598	0.049			
eqQ_1	-1.170	0.039			

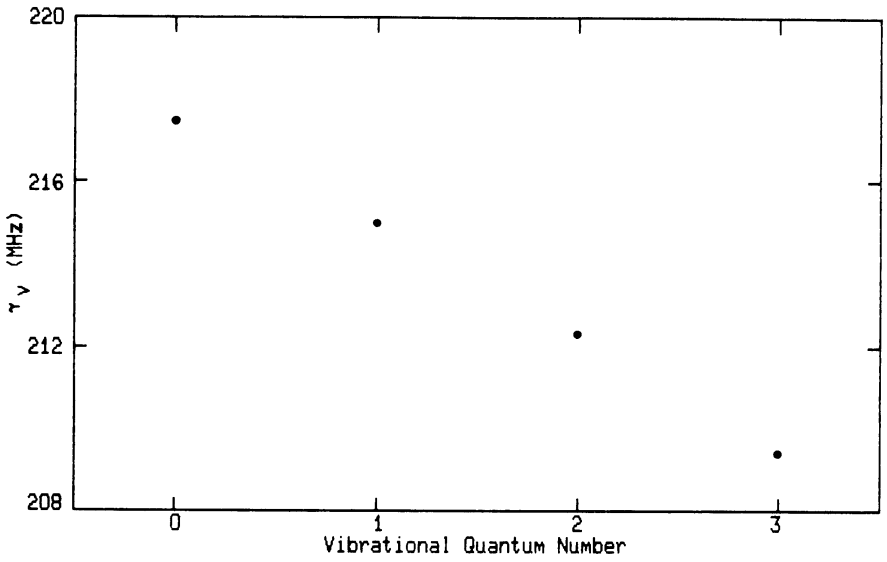

FIG. 3. The spin-rotation constant γ_v as a function of vibrational state. The error bars are too small to show on the resolution of this figure.

The slight mixing associated with the off diagonal J elements is not included in this equation. Recently, Wootten *et al.* have observed $N = 2 \rightarrow 1$ transitions in the shell of IRC + 10216 (*7*). Because these transitions had not been directly observed in the laboratory previous to this work, they calculated these frequencies from the $N = 0 \rightarrow 1$ microwave observations of Dixon and Woods and the optical work of Poletto and Rigutti (*8*). These calculated frequencies differ from ours in large part due to an apparent sign reversal in their use of the nuclear electric quadrupole constant.

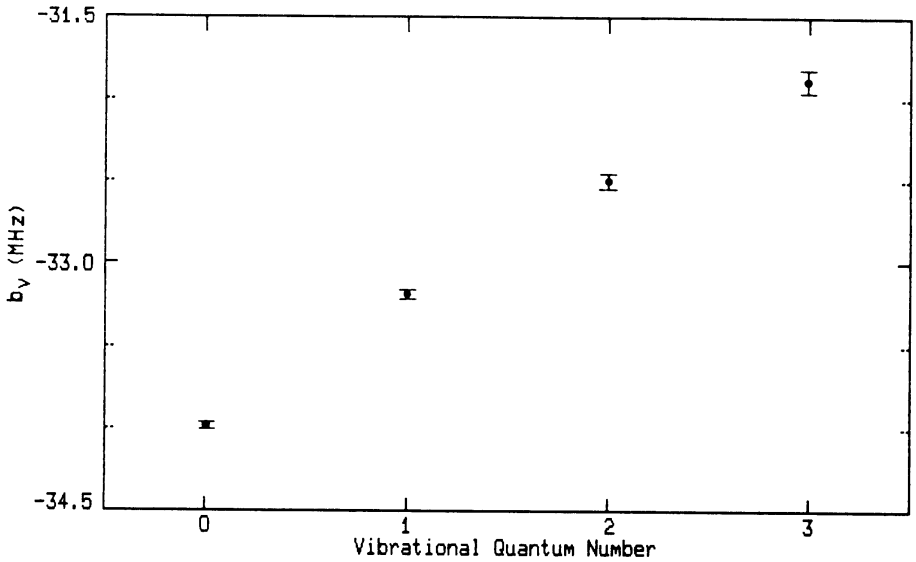

FIG. 4. The magnetic coupling constant b_v as a function of vibrational state. The error bars shown are 1σ.

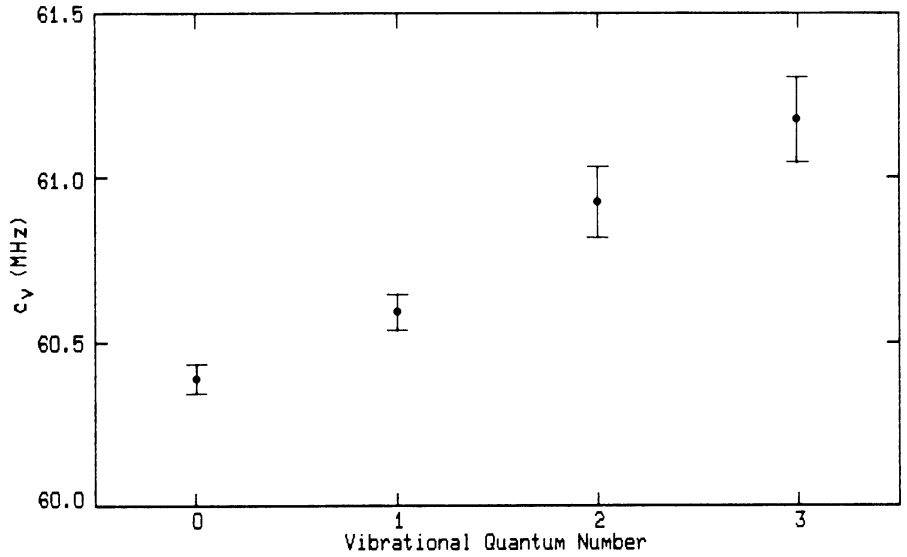

FIG. 5. The magnetic coupling constant c_v as a function of vibrational state. The error bars shown are 1σ.

In addition to the microwave work discussed above, Cenry *et al.* (*9*) have published a detailed analysis of the red system of the CN molecule. For this work they used high resolution Fourier spectroscopy between 4000 and 11 000 cm^{-1}. They observed very high rotational excitation in a number of vibrational states, and were able to calculate a large set of rotation–vibration constants.

Table IV shows a comparison between the calculated B_v and γ_v of their work and the same quantities calculated from our data. For both of the optical constants, it can be seen that the differences between adjacent vibrational states are calculated

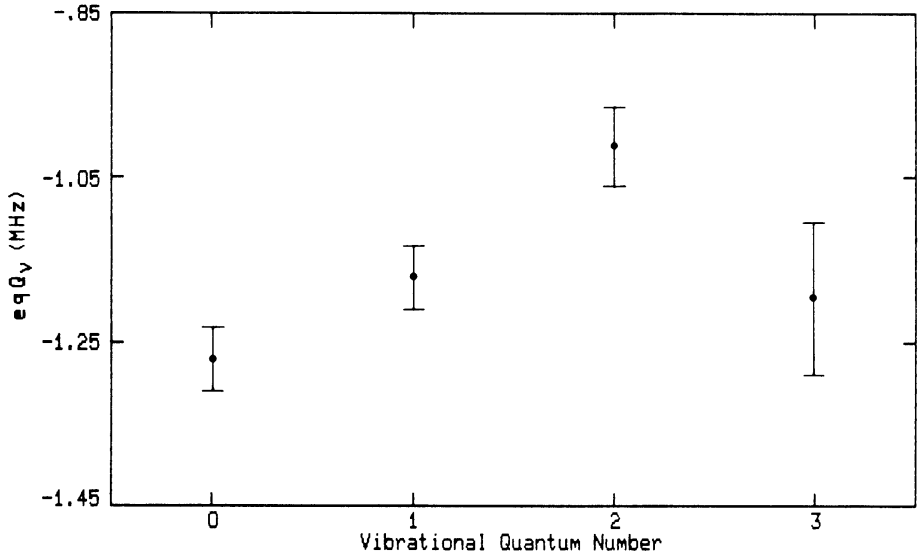

FIG. 6. The electric quadrupole coupling constant eqQ_v as a function of vibrational state. The error bars shown are 1σ.

TABLE III

Calculated Frequencies (MHz) and Relative Intensities

N J F --> N′ J′ F′	INTENSITY	FREQUENCY v = 0	FREQUENCY v = 1	FREQUENCY v = 2	FREQUENCY v = 3
0 1/2 1/2 1 1/2 1/2	1.23	113123.337	112082.120	111037.792	109990.246
0 1/2 1/2 1 1/2 3/2	9.88	113170.502	112128.997	111084.496	110036.768
0 1/2 1/2 1 3/2 1/2	9.88	113499.629	112453.837	111404.580	110352.004
0 1/2 1/2 1 3/2 3/2	12.35	113488.126	112442.792	111393.982	110341.654
0 1/2 3/2 1 1/2 1/2	9.88	113144.122	112101.597	111056.059	110007.457
0 1/2 3/2 1 1/2 3/2	12.35	113191.287	112148.475	111102.763	110053.980
0 1/2 3/2 1 3/2 1/2	1.23	113520.414	112473.315	111422.847	110369.215
0 1/2 3/2 1 3/2 3/2	9.88	113508.911	112462.270	111412.249	110358.865
0 1/2 3/2 1 3/2 5/2	33.33	113490.943	112444.992	111395.574	110342.800
1 1/2 1/2 2 3/2 1/2	4.94	226663.685	224575.590	222481.063	220380.098
1 1/2 1/2 2 3/2 3/2	6.17	226679.341	224591.075	222496.446	220395.238
1 1/2 3/2 2 3/2 1/2	0.62	226616.520	224528.713	222434.358	220333.575
1 1/2 3/2 2 3/2 3/2	4.94	226632.176	224544.197	222449.742	220348.716
1 1/2 3/2 2 3/2 5/2	16.67	226659.543	224571.177	222476.392	220375.145
1 3/2 1/2 2 3/2 1/2	0.62	226287.393	224203.873	222114.274	220018.339
1 3/2 1/2 2 3/2 3/2	0.49	226303.049	224219.357	222129.658	220033.480
1 3/2 1/2 2 5/2 3/2	10.00	226875.896	224785.355	222688.065	220584.071
1 3/2 3/2 2 3/2 1/2	0.49	226298.896	224214.918	222124.873	220028.689
1 3/2 3/2 2 3/2 3/2	1.20	226314.552	224230.402	222140.256	220043.830
1 3/2 3/2 2 3/2 5/2	0.53	226341.919	224257.381	222166.906	220070.259
1 3/2 3/2 2 5/2 3/2	3.20	226887.399	224796.400	222698.663	220594.421
1 3/2 3/2 2 5/2 5/2	16.80	226874.183	224783.640	222686.341	220582.346
1 3/2 5/2 2 3/2 3/2	0.53	226332.519	224247.680	222156.931	220059.896
1 3/2 5/2 2 3/2 5/2	2.80	226359.887	224274.660	222183.581	220086.325
1 3/2 5/2 2 5/2 3/2	0.13	226905.366	224813.678	222715.338	220610.486
1 3/2 5/2 2 5/2 5/2	3.20	226892.151	224800.918	222703.016	220598.412
1 3/2 5/2 2 5/2 7/2	26.67	226874.764	224784.090	222686.665	220582.578
2 3/2 1/2 3 5/2 3/2	6.67	340035.281	336902.301	333759.619	330607.125
2 3/2 3/2 3 5/2 3/2	2.13	340019.625	336886.817	333744.236	330591.984
2 3/2 3/2 3 5/2 5/2	11.20	340035.525	336902.492	333759.757	330607.224
2 3/2 5/2 3 5/2 3/2	0.09	339992.258	336859.838	333717.586	330565.555
2 3/2 5/2 3 5/2 5/2	2.13	340008.158	336875.513	333733.107	330580.795
2 3/2 5/2 3 5/2 7/2	17.78	340031.567	336898.513	333755.746	330603.205
2 5/2 3/2 3 5/2 3/2	0.53	339446.779	336320.819	333185.829	330041.393
2 5/2 3/2 3 5/2 5/2	0.10	339462.679	336336.494	333201.350	330056.633
2 5/2 3/2 3 7/2 5/2	12.70	340248.573	337113.200	333967.786	330812.395
2 5/2 5/2 3 5/2 3/2	0.10	339459.994	336333.579	333198.151	330053.468
2 5/2 5/2 3 5/2 5/2	0.75	339475.894	336349.254	333213.672	330068.708
2 5/2 5/2 3 5/2 7/2	0.10	339499.303	336372.255	333236.312	330091.118

N J F --> N' J' F'	INTENSITY	FREQUENCY	FREQUENCY	FREQUENCY	FREQUENCY
		v = 0	v = 1	v = 2	v = 3
2 5/2 5/2 3 7/2 5/2	1.55	340261.788	337125.960	333980.109	330824.470
2 5/2 5/2 3 7/2 7/2	17.49	340247.625	337112.249	333966.830	330811.437
2 5/2 7/2 3 5/2 5/2	0.10	339493.281	336366.082	333230.023	330084.541
2 5/2 7/2 3 5/2 7/2	1.17	339516.690	336389.083	333252.663	330106.952
2 5/2 7/2 3 7/2 5/2	0.03	340279.175	337142.788	333996.460	330840.303
2 5/2 7/2 3 7/2 7/2	1.55	340265.012	337129.077	333983.181	330827.271
2 5/2 7/2 3 7/2 9/2	23.81	340247.874	337112.442	333966.968	330811.537
3 5/2 3/2 4 7/2 5/2	9.52	453391.571	449213.775	445022.978	440819.089
3 5/2 5/2 4 7/2 5/2	1.17	453375.671	449198.101	445007.457	440803.850
3 5/2 5/2 4 7/2 7/2	13.12	453391.708	449213.881	445023.054	440819.144
3 5/2 7/2 4 7/2 5/2	0.02	453352.262	449175.100	444984.817	440781.439
3 5/2 7/2 4 7/2 7/2	1.17	453368.299	449190.881	445000.415	440796.733
3 5/2 7/2 4 7/2 9/2	17.86	453390.011	449212.176	445021.336	440817.422
3 7/2 5/2 4 7/2 5/2	0.36	452589.777	448421.395	444241.021	440048.088
3 7/2 5/2 4 7/2 7/2	0.03	452605.814	448437.176	444256.618	440063.382
3 7/2 5/2 4 9/2 7/2	13.89	453607.236	449427.033	445233.498	441026.699
3 7/2 7/2 4 7/2 5/2	0.03	452603.940	448435.106	444254.300	440061.120
3 7/2 7/2 4 7/2 7/2	0.46	452619.977	448450.887	444269.897	440076.414
3 7/2 7/2 4 7/2 9/2	0.03	452641.689	448472.182	444290.818	440097.103
3 7/2 7/2 4 9/2 7/2	0.91	453621.399	449440.744	445246.777	441039.732
3 7/2 7/2 4 9/2 9/2	17.60	453606.634	449426.429	445232.890	441026.090
3 7/2 9/2 4 7/2 7/2	0.03	452637.115	448467.522	444286.109	440092.149
3 7/2 9/2 4 7/2 9/2	0.63	452658.827	448488.817	444307.030	440112.837
3 7/2 9/2 4 9/2 7/2	0.01	453638.537	449457.379	445262.989	441055.466
3 7/2 9/2 4 9/2 9/2	0.91	453623.772	449443.064	445249.102	441041.824
3 7/2 9/2 4 9/2 11/2	22.22	453606.772	449426.536	445232.967	441026.145

TABLE IV

Comparison of Microwave and Optical Results (MHz)

Constant	Microwave	Optical	Difference
B_0	56693.461(3)	56693.256(129)	0.205
B_1	56171.110(5)	56170.910(132)	0.200
B_2	55647.106(5)	55646.905(132)	0.201
B_3	55121.435(15)	55121.183(141)	0.252
γ_0	217.500(5)	222.36(99)	-4.86
γ_1	215.071(12)	220.86(99)	-5.79
γ_2	212.332(18)	218.01(138)	-5.68
γ_3	209.386(57)	215.55(135)	-6.16

much more accurately than the absolute values. The major disagreement between the microwave and optical γ_v has been previously noted in Ref. (*9*). Since the microwave values are calculated very directly from a substantially redundant and highly accurate data set, we assume them to be correct. It should be noted that the comparison shown in Ref. (*9*) between the optical and the microwave B_0 is in fact a comparison between the microwave $B'_0 \equiv B_0 - 2D_0$ and an optical B_0. B'_0 is the microwave constant available from the previous microwave work which included only $N = 1 \leftarrow 0$ transitions.

The optical data set was fit to a somewhat different model, so a direct comparison of their derived "equilibrium" constants and our "Dunham" constants is not possible. This is not because we identify the coefficients of the power series as Dunham constants and they identify them as equilibrium constants, but rather because we retain different constants and use different fitting procedures. Even though a direct comparison between our Y_{01} and the B_e of Ref. (*9*) is not strictly appropriate, the large disagreement between the optical B_e (56 953.816(7) MHz) and our Y_{01} (56 954.023(5) MHz) is probably due to a misprint in the place value of the uncertainty in Table V of Ref. (*9*). This would increase their uncertainty by an order of magnitude and place the disagreement at the 3σ rather than 30σ level.

RECEIVED: November 15, 1982

REFERENCES

1. H. E. RADFORD AND H. P. BROIDA, *Phys. Rev.* **128,** 231–242 (1962); H. N. KIESS AND H. P. BROIDA, *J. Mol. Spectrosc.* **7,** 194–208 (1961); T. J. COOK AND D. H. LEVY, *J. Chem. Phys.* **58,** 3547–3557 (1973); J. M. WEINBERG, E. S. FISHBURNE, AND K. NARAHARI RAO, *J. Mol. Spectrosc.* **22,** 406–418 (1967).
2. A. A. PENZIAS, R. W. WILSON, AND K. B. JEFFERTS, *Phys. Rev. Lett.* **32,** 701–704 (1974).
3. T. A. DIXON AND R. C. WOODS, *J. Chem. Phys.* **67,** 3956–3964 (1977).
4. P. HELMINGER, F. C. DE LUCIA, AND W. GORDY, *Phys. Rev. Lett.* **25,** 1397–1399 (1970).
5. W. W. CLARK AND F. C. DE LUCIA, *J. Chem. Phys.* **74,** 3139–3147 (1981).
6. R. L. COOK AND F. C. DE LUCIA, *Amer. J. Phys.* **39,** 1433–1454 (1971).
7. A. WOOTTEN, S. M. LICHTEN, R. SAHAI, AND P. G. WANNIER, *Astrophys. J.* **257,** 151–160 (1982).
8. G. POLETTO AND M. RIGUTTI, *Nuovo Cimento* **39,** 519–530 (1965).
9. D. CERNY, R. BACIS, G. GUELACHVILI, AND F. ROUX, *J. Mol. Spectrosc.* **73,** 154–167 (1978).